J|A|C|S COMMUNICATIONS

Published on Web 01/07/2009

Site-Specific Immobilization and Micrometer and Nanometer Scale Photopatterning of Yellow Fluorescent Protein on Glass Surfaces

Nicholas P. Reynolds,[†] Jaimey D. Tucker,[‡] Paul A. Davison,[‡] John A. Timney,[‡] C. Neil Hunter,[‡] and Graham J. Leggett*,[†]

Department of Chemistry, University of Sheffield, Brook Hill, Sheffield S3 7HF, U.K., and Department of Molecular Biology and Biotechnology, University of Sheffield, Western Bank, Sheffield S10 2TN, U.K.

Received October 7, 2008; E-mail: graham.leggett@sheffield.ac.uk

The development of methods for molecular patterning with nanoscale spatial resolution remains a significant challenge in the burgeoning field of bionanotechnology. While there has been a great deal of progress in the development of techniques based on scanning probe microscopy, such as dip-pen nanolithography,[1−6] nanoshaving/grafting,[7] and near-field optical methods,[8−10] much work has focused on nucleic acids, and there are fewer reports of protein patterning. Moreover, much work has also utilized self-assembled monolayers (SAMs) of alkanethiols on gold as templates for molecular patterning. In addition to a limited stability, they suffer the disadvantage that gold quenches optical activity, rendering the interrogation of biomolecules by spectroscopic techniques more difficult. From the perspective of applications in biology, nanostructures formed on oxide surfaces are particularly attractive,[11] and the oxide of choice would be, in many cases, glass. There have been comparatively few attempts to fabricate nanostructures on silicon dioxide, with the development of constructive nanolithography by Sagiv and co-workers being the most extensive effort to date in this direction.[12,13]

In a previous study, it was demonstrated that UV exposure of tri(ethylene glycol) terminated alkanethiol SAMs caused their degradation to yield surface aldehyde groups, which covalently bound amines and proteins.[14] Here we report a development that should facilitate the nanometer-scale patterning of any histidine-tagged protein on glass. It is shown first, that an oligo(ethylene glycol) (OEG) terminated siloxane monolayer on glass may be degraded by UV light to yield aldehyde groups; second, that these may be used to immobilize nitrilo(triacetic acid) terminated amines, facilitating site-specific immobilization of His-tagged proteins;[6] and third, that combination of this method with near-field exposure yields sub-200 nm structures that may be imaged by confocal microscopy to yield diffraction-limited images.

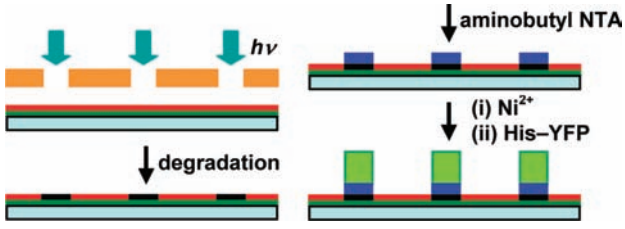

Figure 1. Schematic diagram representing the process used to immobilize His-YFP.

The method is shown schematically in Figure 1. A glass surface was immersed in a solution of mercaptopropyltrimethoxysilane (MPTMS) in tetrahydrofuran yielding a mercaptosilane-functionalized substrate that was then derivatized with methyl-PEO_{12}-maleimide (PEO = poly(ethylene oxide)), yielding a protein-resistant surface. The sample was exposed to UV light from a frequency-doubled argon ion laser (244 nm) through a mask or, for nanometer scale patterning, using a scanning near-field optical microscope. In exposed areas, EO groups were degraded to yield aldehydes. Samples were then placed in a solution of *N*-[5-(3′-maleimidopropylamido)-1-carboxypentyl] iminodiacetic acid in deionized water, yielding a nitrilotriacetic acid terminated surface which, following exposure to a solution of nickel ions was able to bind proteins. The protein used here was histidine-tagged yellow fluorescent protein (His-YFP, see Supporting Information for details of its preparation).

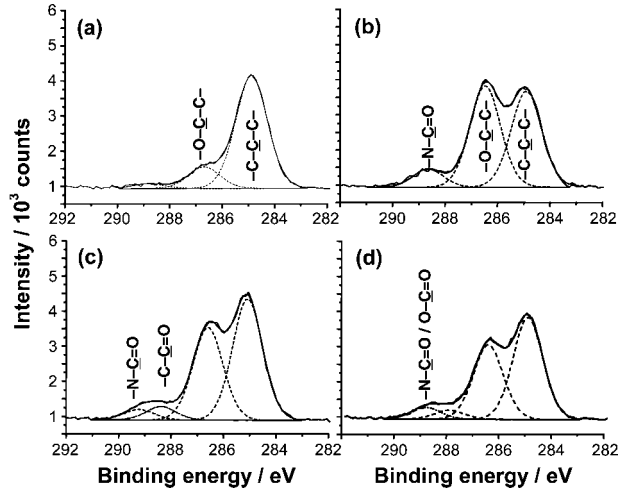

Figure 2. C1s XPS spectra of MPTMS films on glass: (a) virgin monolayer; (b) after derivatization with methyl-PEO_{12}-maleimide; (c) after subsequent exposure to UV light (7.6 J cm^{-2}); and (d) after further derivatization with *N*-(5-amino-1-carboxypentyl)iminoacetic acid.

X-ray photoelectron spectroscopy (XPS) was used to characterize the surface attachment chemistry (Figure 2). The C1s spectrum of the MPTMS film (Figure 2a) exhibited a peak at 285 eV corresponding to the aliphatic carbon atoms in the propyl chain, together with a small ether peak, attributed to unreacted methoxy groups. Following derivatization with methyl-PEO_{12}-maleimide, the ether component became the dominant one in the spectrum (Figure 2b) and a peak was observed at 288.9 eV due to the imide carbon atoms. Exposure to 7.6 J cm^{-2} UV light (Figure 2c) led to a reduction in the intensity of the ether peak, and the appearance of a new peak 288.2 eV attributed to the formation of aldehydes. These data indicate that the PEO functionalized siloxane film undergoes a similar degradation process to the one reported previously for OEG functionalized alkanethiol SAMs.[14] Doubling the exposure yielded

[†] Department of Chemistry.
[‡] Department of Molecular Biology and Biotechnology.

10.1021/ja8079252 CCC: $40.75

a further reduction in the size of the ether component, but no further increase in the area of the aldehyde peak, suggesting that a steady-state composition was reached at the lower UV exposure, and that subsequently, gradual degradation of the PEO chain occurs without significant alteration of the composition. Following UV exposure, samples were immersed in a solution of *N*-(5-amino-1-carboxypentyl)iminoacetic acid (AB-NTA), which reacted with aldehyde groups, via imine bond formation, yielding an NTA-terminated surface. This led to an increase in the size of the component in the C1s spectrum at 288.9 eV (Figure 2d).

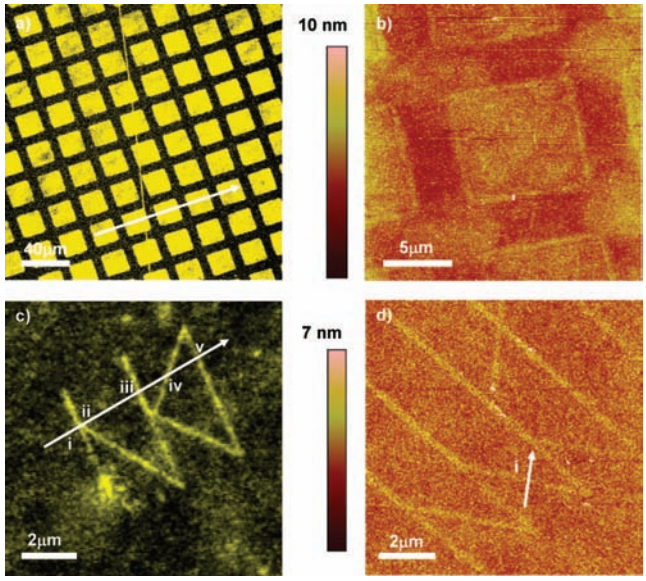

Figure 3. His-tagged YFP bound to photodegraded, NTA-functionalized PEO-terminated films: (a) confocal microscopy image of a micrometer-scale pattern of YFP formed by exposure through a mask; (b) tapping mode AFM image of the same pattern; (c) confocal microscopy image; and (d) tapping mode AFM image of nanolines of YFP formed by SNP. Line sections through the images are shown in the Supporting Information.

Patterned samples were prepared by exposure through a mask and subsequent immersion in a solution of AB-NTA. The samples were then exposed to an aqueous solution of $NiSO_4$, leading to complexation of the NTA-functionalized regions by Ni^{2+}, and finally a solution of His-tagged YFP in buffer. Confocal microscopy was used to measure the fluorescence of the resulting patterns (Figure 3a). High contrast was observed, with bright fluorescence being observed for the exposed regions (squares), indicating high levels of attachment, and dark contrast in the masked areas (bars), indicating very low levels of nonspecific adsorption on the intact OEG-functionalized regions. Treatment of the samples with a solution of imidazole, which is able to disrupt interactions between nickel-NTA complexes and His-residues, led to a complete loss of fluorescence, indicating that the protein binding was via site-specific binding to His residues rather than nonspecific physisorption to the NTA-functionalized surfaces. Tapping mode AFM topographical images supported these conclusions. Figure 3b shows a representative image. Uniform contrast was observed over the exposed regions, which exhibited a mean height of ca. 1 nm, consistent with the attachment of a monolayer of protein molecules. The regions between exposed areas were free of nonspecifically adsorbed protein (see also Figure 1 in Supporting Information for high magnification fluorescence image) although deposits of material from the buffer solution were observed to form during drying, particularly at intersections between masked regions (bars).

Smaller structures were fabricated using scanning near field photolithography (SNP), in which the UV laser is coupled to a scanning near-field optical microscope. The near-field probe was traced across the sample, causing photodegradation of the PEO-terminated siloxane film, and the sample was then treated in exactly the same way that the micropatterned samples were treated, by first immersing it in AB-NTA, then nickel sulfate solution, and finally the YFP solution. Confocal fluorescence images yielded good contrast, although at long exposures, photobleaching was a problem. A cross-section through the confocal microscope image of the YFP nanolines yielded a mean full width at half-maximum height (fwhm) of 393 nm. However, the longer lines (i, iii, and v in Figure 3c) resulted from two sweeps by the probe, and were subject to broadening due to piezo hysteresis. On the diagonals (single-sweeps, ii and iv), a fwhm of 262 nm was measured. The tapping mode image showed no evidence of nonspecific adsorption (Figure 3d). The fwhm of the diagonal was found to be 179 nm, close to the diameter of the aperture in the probe used (150 nm), and somewhat smaller than the dimensions measured by confocal microscopy, indicating that the resolution in Figure 3c was limited by the resolving power of the confocal microscope. The height of the line was measured to be 0.8 nm, indicating the formation of a monolayer of site-specifically bound protein (see Supporting Information). Together, Figure 3 panels c and d confirm that using very simple photochemical methods, it is feasible to fabricate protein nanostructures on glass that retain high levels of optical activity, enabling characterization by readily available confocal microscopy equipment.

While the present study has focused on the patterning of YFP, the method described here should have widespread applicability because of the comparative ease with which His residues can be introduced in a site-specific way to a large variety of proteins. The capacity to fabricate structures smaller than the diffraction limit of optical microscopy, that may nevertheless be conveniently characterized optically without fluorescence quenching, is important for potential applications in bionanotechnology.

Acknowledgment. N.P.R. thanks Miss M. Charnley and Dr. G. Fowler for assistance using the confocal microscope and the EPSRC for a Life Sciences Doctoral Training Centre Studentship. J.T., C.N.H., and G.J.L. acknowledge BBSRC for support.

Supporting Information Available: Line sections through the images in Figure 3a,c,d and a high magnification fluorescence image of a micropatterned sample. This material is available free of charge via the Internet at http://pubs.acs.org.

References

(1) Piner, R. D.; Zhu, J.; Xu, F.; Hong, S.; Mirkin, C. A. *Science* **1999**, *283*, 661.
(2) Demers, L.; Ginger, D. S.; Park, S.-J.; Li, Z.; Chung, S.-W.; Mirkin, C. A. *Science* **2002**, *296*, 1836.
(3) Lee, K.-B.; Park, S.-J.; Mirkin, C. A.; Smith, J. C.; Mrksich, M. *Science* **2002**, *295*, 1702.
(4) Hyun, J.; Ahn, S. J.; Lee, W. K.; Chilkoti, A.; Zauscher, S. *Nano Lett.* **2002**, *2*, 1203.
(5) Lee, K.-B.; Lim, J.-H.; Mirkin, C. A. *J. Am. Chem. Soc.* **2003**, *125*, 5588.
(6) Nam, J-W.; Han, S. W.; Lee, K.-B.; Liu, X.; Ratner, M. A.; Mirkin, C. A. *Agnew. Chem. Int. Ed.* **2004**, *43*, 1246.
(7) Liu, G.-Y.; Amro, N. A. *Proc. Natl. Acad. Sci. U.S.A.* **2002**, *99*, 5165.
(8) Sun, S.; Montague, M.; Critchley, K.; Chen, M.-S.; Dressick, W. J.; Evans, S. D.; Leggett, G. J. *Nano Lett.* **2006**, *6*, 29.
(9) Montague, M.; Ducker, R. E.; Chong, K. S. L.; Manning, R. J.; Rutten, F. J. M.; Davies, M. C.; Leggett, G. J. *Langmuir* **2007**, *23*, 7328.
(10) Reynolds, N. P.; Janusz, S. J.; Escalante-Marun, M.; Timney, J.; Ducker, R. E.; Olsen, J. D.; Otto, C.; Subramanian, V.; Leggett, G. J.; Hunter, C. N. *J. Am. Chem. Soc.* **2007**, *129*, 14625.
(11) Nam, J.-M.; Han, S. W.; Lee, K.-B.; Liu, X.; Ratner, M. A.; Mirkin, C. A. *Angew. Chem., Int. Ed.* **2004**, *43*, 1246.
(12) Maoz, R.; Frydman, E.; Cohen, S. R.; Sagiv, J. *Adv. Mater.* **2000**, *12*, 725.
(13) Hoeppener, S.; Maoz, R.; Sagiv, J. *Nano Lett.* **2003**, *3*, 761.
(14) Ducker, R. E.; Janusz, S. J.; Sun, S.; Leggett, G. J. *J. Am. Chem. Soc.* **2007**, *129*, 14842.

JA8079252